Novelty imaging system with a desired long-time scale using $BaTiO_3$ and a controlled shutter sequence

Takamasa Suzuki and Takuso Sato

A novelty imaging system using photorefractive crystal $BaTiO_3$ and a controlled shutter sequence, which can be applied to the slow-motion detection of the object, is proposed. In this system the observation time scale is set to the desired long value uninfluenced by the time constant of the crystal that is used. This system utilizes a photorefractive beam-fanning effect in the $BaTiO_3$ crystal, so it is constructed simply by using only the object beam without suffering from the external disturbance that is intrinsic when the reference beam is used. Moreover, the visibility for an opaque object is also maintained by the use of an additional random-phase plate. We examine the basic characteristics and determine the appropriate conditions of the system.

I. Introduction

Motion detection, which in a sense is temporal high-pass filtering, is one of the basic visual functions of animals, and this has been studied for years as a novelty filter[1] in the visual neural network. The detection of changes in the object, for example, changes of position or shape of parts, can be performed electrically by subtracting a stored image from the current image.[2] When an optical technique is used, this process is performed in parallel and real time with a simple system, while an electrical method needs a long time for serial calculation and large-size memories. Moreover, the phase changes can be detected by an optical system.

Until now, novelty filters that use a photorefractive effect such as phase conjugation,[3] two-beam coupling,[4-7] and beam fanning[8] have been proposed. These systems detect only the images which change within a response time of the photorefractive crystal itself, a crystal such as BSO or $BaTiO_3$. Recently a novelty filter that copes with a high-speed object was proposed, and the resolution was examined.[9] But it is difficult for these novelty filters to detect clearly the changes in low-speed objects when these changes within the response time of the crystal are slight. One way to overcome this problem is to control the beam intensity following the speed of the object, because the response time depends on the intensity of the incident beam. But this may be troublesome and disadvantageous for visibility.

Here we propose an extended form of a novelty imaging system that can operate on the desired long-time scale by using a controlled shutter sequence by which the slow motion of the object can be observed clearly. Our system uses only the object beam, in connection with the beam-fanning effect,[10-12] to simplify the construction and to make it more robust for disturbances. Moreover, we examine experimentally the effect of the use of a random phase plate to keep visibility for an opaque object.

II. Principle

A. Beam-Fanning in $BaTiO_3$

Our system uses the beam-fanning effect of the photorefractive crystal, $BaTiO_3$. The process is explained in Fig. 1. The source of the effect is the interference of an incident object beam $I_i(t)$ and a fractional noise beam $I_s(t)$ scattered from $I_i(t)$ (shown in Fig. 1). That is to say, two-beam coupling[13-17] occurs in the crystal. The interference pattern introduces the static electric field in the crystal, which makes a phase hologram. The energy is transferred to the scattered beam $I_s(t)$ from the object beam $I_i(t)$ through the hologram. Consequently, the intensity of the fanning beam $I_f(t)$ is amplified and the output $I_o(t)$

T. Suzuki is with the Faculty of Engineering, Niigata University, 8050 Ikarashi 2, Niigata-shi 950-21, Japan. T. Sato is with the Graduate School at Nagatsuta, Tokyo Institute of Technology, 4259 Nagatsuta, Midoriku, Yokohama 227, Japan.

Received 6 April 1991.
0003-6935/92/050606-07$05.00/0.

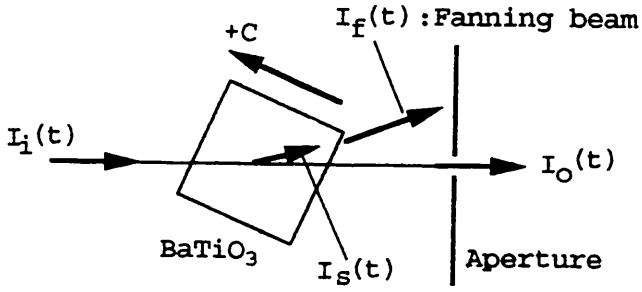

Fig. 1. Configuration of beam fanning in $BaTiO_3$. $I_s(t)$ is a fractional noise scattered from the incident object beam $I_i(t)$. $I_f(t)$ is an amplified fanning beam, and $I_o(t)$ is an energy-depleted output object beam.

is depleted when the incident beam $I_i(t)$ has a constant intensity of $I_i(0)$. The output beam intensity $I_o(t)$ is given by[11]

$$I_o(t) = \frac{1 + m_0}{1 + m_0 \exp[\Gamma(t)L]} I_i(0), \tag{1}$$

where $m_0 = I_s(0)/I_i(0)$ is the initial scattering ratio, L is the beam interaction length, and $\Gamma(t)$ is the beam coupling strength, given by

$$\Gamma(t) = \Gamma_0[1 - \exp(-t/\tau_h)], \tag{2}$$

where Γ_0 is a maximum gain coefficient of the crystal, and τ_h is a time constant for the formation of the phase hologram. To be accurate, the evolution of the output beam $I_o(t)$ follows Eq. (1), but it shows experimentally the quasi-exponential evolution, as shown in Ref. 11. So we make a rough approximation for $I_o(t)$ and $I_f(t)$ as follows:

$$I_o(t) = I_i(0) \exp(-t/\tau) + I_{offset}, \tag{3}$$

$$\begin{aligned} I_f(t) &= I_i(0) - I_o(t) \\ &= I_i(0)[1 - \exp(-t/\tau)] - I_{offset}, \end{aligned} \tag{4}$$

where I_{offset} is an offset beam intensity that is not contributed by the energy transfer and τ is a time constant decided from the experimental results. The above approximation is useful to discuss the resolution of our system without any serious error resulting. We use only the object beam by removing the fanning beam $I_f(t)$ with an aperture as shown in Fig. 1.

B. Control of the Time Constant with Shutter

Let us consider an object that has a uniform phase distribution. Figure 2 shows the configuration of the motion detection.

If the object is stationary the detected image is dark, as shown in Fig. 2(a), because the phase hologram generated in $BaTiO_3$ matches the phase of the incident beam and the energy of the object beam is almost transferred to the fanning beam. But we can detect only the part whose phase is mismatched with a phase hologram in $BaTiO_3$ when the object moves. If

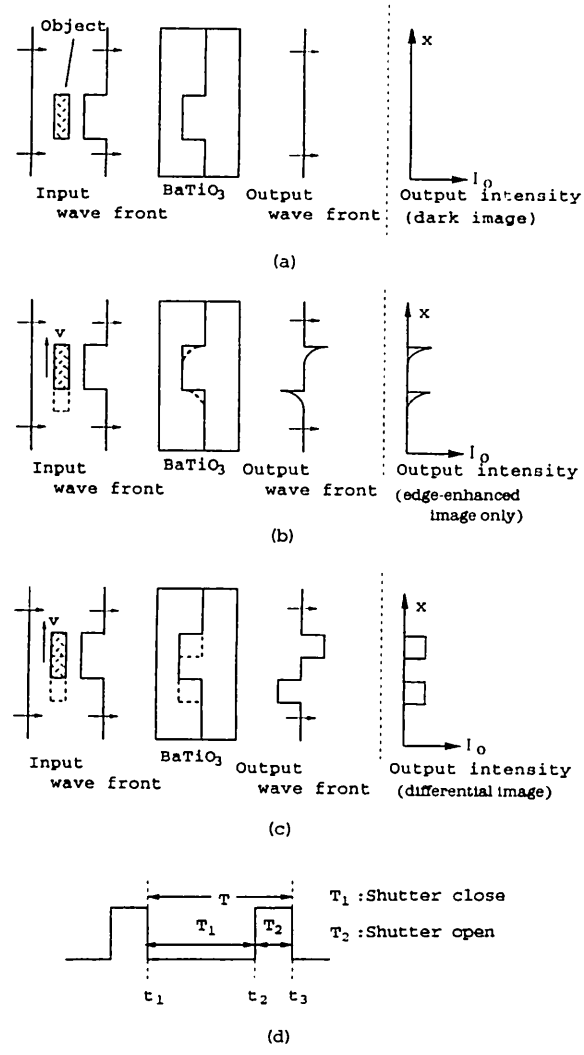

Fig. 2. Image detection (a) at steady state, (b) without a shutter, and (c) with a shutter with control sequence (d).

the object moves in the x direction by the distance L with a constant speed v, the normalized intensity of the detected image is expressed by

$$\begin{aligned} I_d(x) &= I_o[(L - x)/v]/I_i(0) \\ &= \exp[-(L - x)/v\tau], \end{aligned} \tag{5}$$

where I_{offset} is ignored and $(L - x)/v$ denotes a time required for the movement. Therefore the normalized average intensity I_a in the changed area is obtained by

$$\begin{aligned} I_a &= \frac{1}{L} \int_0^L I_d(x)dx \\ &= (\tau/T)\,[1 - \exp(-T/\tau)], \end{aligned} \tag{6}$$

where $T = L/v$. Equation (6) shows that the average intensity depends on the object's speed and time constant τ. When the speed v is as small as $L/v > \tau$, it is clear that I_a becomes small and the detected image is almost dark. Moreover, since the hologram is regenerated continuously, we can detect only the

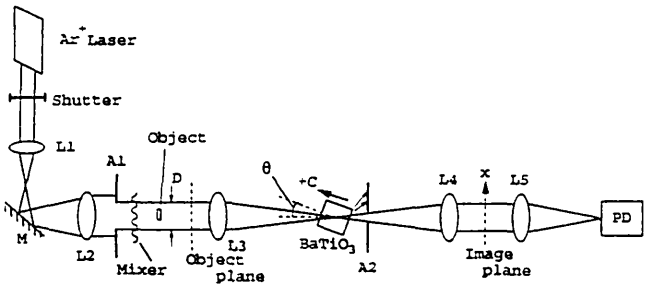

Fig. 3. Experimental setup: M, mirror; A1, A2, apertures; L1-L5, lenses; PD, photodetector.

edge-enhanced image shown in Fig. 2(b), even if the object's speed is as large as $L/v < \tau$. To overcome this problem, we use a controlled shutter. If we controll the shutter periodically, as shown in Fig. 2(d), we can detect the difference between the images at times t_1 and t_2, becuase the phase hologram, which has been generated at time t_1, is kept at time t_2. In this way, the equivalent time constant of the photorefractive crystal can be adjusted to the desired large value T ($T \gg \tau$). It is required that the shutter-opening period T_2 be greater than τ in order to regenerate the phase hologram broken at $t = t_2$. The output image becomes dark again at $t = t_3$.

C. Improvement of Contrast for Opaque Objects

When an object is opaque, the image at the position where it was placed just before movement can be detected clearly because the position where the beam had been intercepted is irradiated by the incident beam. But it is difficult to see the object image clearly at the position just after movement because there is little diffracted light behind it. So we introduce a random-phase plate as the mixer. It increases the diffraction and both images of the object can be observed clearly.

III. Experimental Results

A. Experimental Setup

The experimental setup is shown in Fig. 3. An argon-ion laser (λ = 514.5 nm) is used as the light source. The beam is expanded with lenses $L1$ and $L2$ after the shutter. The expanded beam irradiates the object. The mixer is a transparent plastic plate which has a random phase distribution and is used when the object is opaque. The photorefractive crystal $BaTiO_3$ is placed at the Fourier plane, and the object beam is introduced to it by lens $L3$. The beam is ~2 mm in diameter and intersects the c axis by an angle θ in the crystal. The crystal size is 5 mm × 5 mm × 5 mm. The object beam, which has passed the crystal, is imaged onto the CCD video camera with a lens L_4 at the image plane after cutting the fanning beam by the aperture $A2$.

B. Basic Characteristics of the System

The dependence of the output beam intensity on the beam incident angle θ is measured. The incident

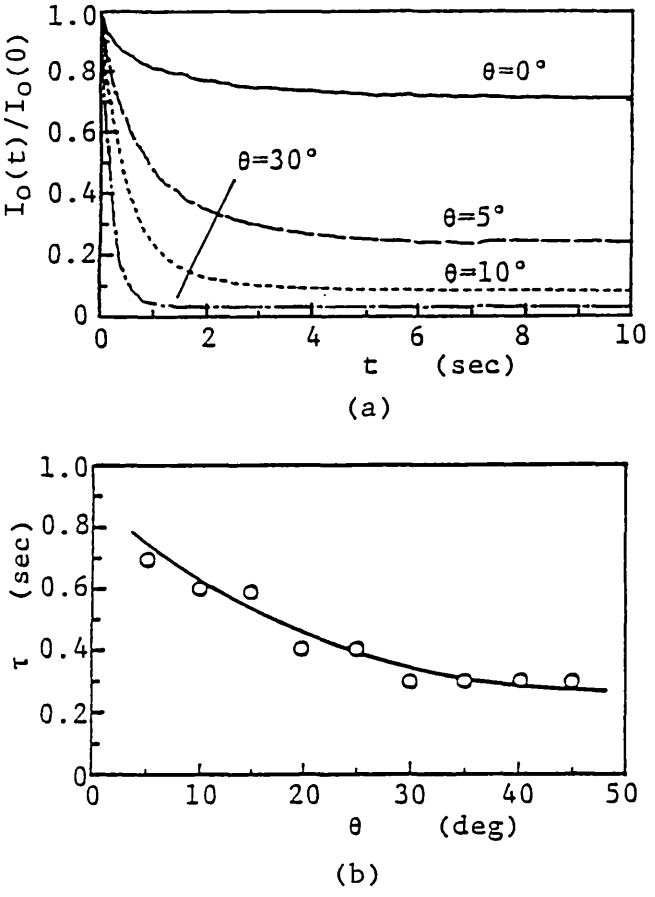

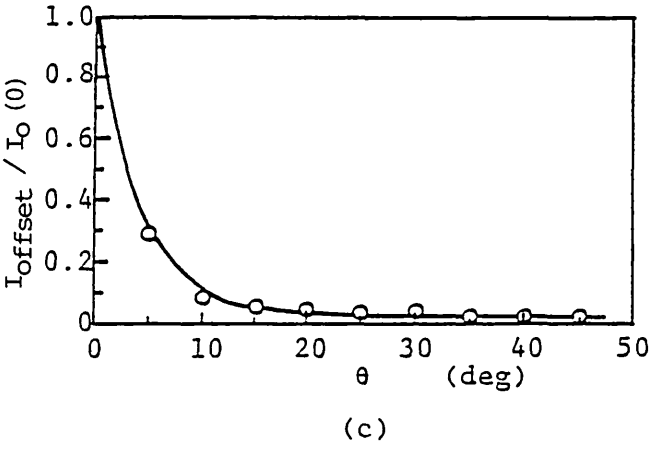

Fig. 4. Dependence of (a) the evolutions of normalized output beam intensity, (b) the time constant of the system, and (c) the steady-state normalized output beam intensity on the beam incident angle θ.

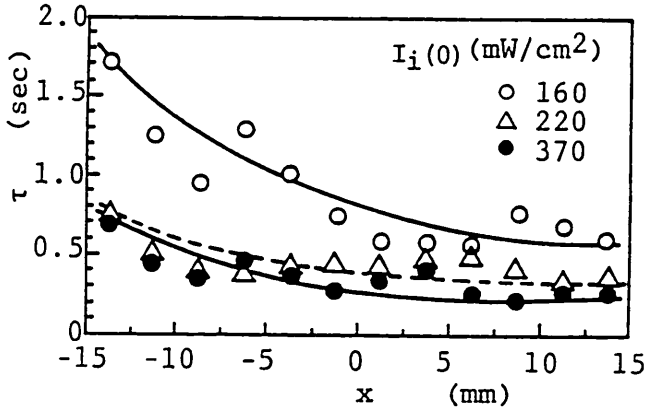

Fig. 5. Distributions of time constants along the x axis in an image plane.

beam intensity is constant and its power is ~300 mW/cm². The results are shown in Fig. 4. Figure 4(a) shows the evolutions of the output beam intensities for various incident angles. The values are normalized by the output beam initial intensities. It is seen that the intensity decreases exponentially, as given by Eq. (3). Figure 4(b) shows the time constant τ calculated from Fig. 4(a). The time constant is defined as the time required for the intensity to drop to $1/e$ of its initial value. It is seen that τ is reduced with the increase of θ and reaches a constant for $\theta > 30°$. The steady-state intensities in Fig. 4(a) are also plotted in Fig. 4(c). The values are normalized with the value at $\theta = 0°$. It shows that the steady-state intensity becomes a constant and the incident beam is depleted by ~97% of its energy for $\theta > 25°$. Because of these results, $\theta = 30°$ is adopted in the following experiments.

The beam fanning seems to occur asymmetrically with respect to the x axis, as shown in Fig. 3. The measured time constant τ, as a function of the incident beam intensity, is shown in Fig. 5. When the incident beam is weak, τ decreases with the increase of the x coordinate, since the beam fanning starts from the positive x direction. But if the incident beam is stronger than 220 mW/cm², τ is almost constant over the entire measuring region. So the incident beam power that we use is 300 mW/cm².

In our system, the incident object beam is interrupted by a shutter after the generation of the hologram; hence the hologram holding characteristic is an important factor. We examined it by using the constant incident beam and the shutter sequence as shown in Fig. 6(a). I_m is the maximum output beam intensity measured when the zero hologram is generated in the crystal. When I_m is depleted to I_{offset} after a sufficient period of time T_w, the shutter is closed. The shutter closing time is T_h. The output beam intensity rises to I_r just after opening the shutter. The hologram holding coefficient K_h is defined by

$$K_h = [I_m - (I_r - I_{offset})]/I_m, \tag{7}$$

and $K_h = 1$ is ideal for our system. Figure 6(b) shows the measured K_h values. It is seen that K_h is kept at ~1 for $T_h < 500$ s.

A moving, thin glass plate was observed as the object to examine the advantage of the use of a shutter. The object was moved toward the x direction by using various velocities [v(mm/s)] and was measured at the time when the image was overlapped by only $L = 2$ mm. We used an averaged intensity I_a in a square 2 mm × 2 mm of the observed image to estimate quantitatively the difference of the intensity. The measurement results are shown in Fig. 7. I_a is normalized by its maximum value. Images (i)–(iii) and (iv) and (v) were measured without a shutter and with a shutter, respectively. The shutter closing period was given by $T = L/v$ and the shutter opening period was selected as 1 s for the hologram to be regenerated completely. When the shutter was not used, the output images became dark as its speed decreased, as discussed in Section II. The measure-

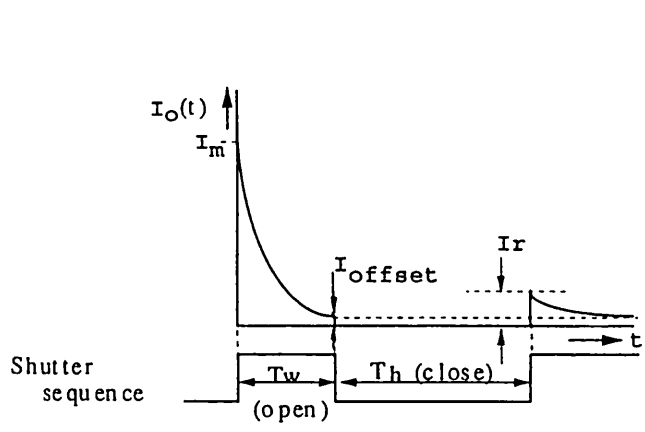

(a)

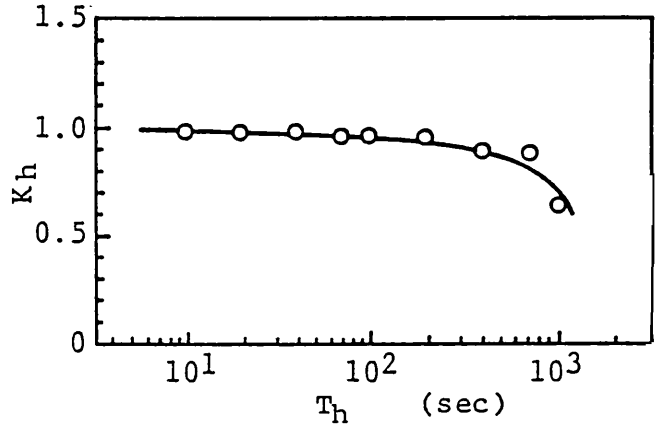

(b)

Fig. 6. Holding characteristic of the phase hologram in a dark state. (a) Change of the output beam intensity corresponding to the shutter sequence, (b) the measured result.

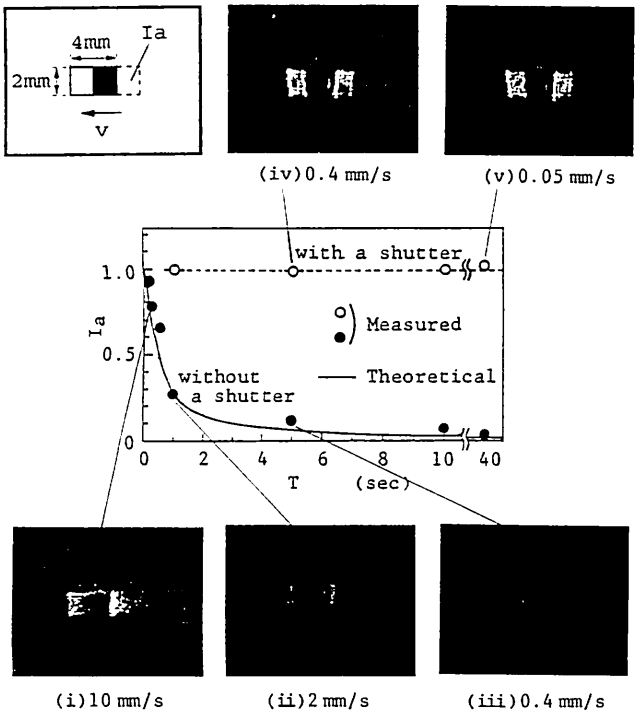

Fig. 7. Images observed: (i)–(iii) without a shutter, (iv)–(v) with a shutter; normalized intensity I_a shown in the inset.

ment values agree well with the theoretical line calculated from Eq. (6) for $\tau = 0.3$ s, shown in Fig. 7. Images (i)–(iii) show that (i) the changed part cannot be obtained clearly, even if the speed is comparatively large, (ii) only the edge part can be detected at low spead, and (iii) the image cannot be obtained at all at a low speed. If we cut the incident object beam by using a shutter, the changed part in the shutter closing period could be detected clearly like images (iv) or (v) of Fig. 7, even if the speed v were small.

In our system, the reference beam is served from the original object beam, so the size ratio of the area between changed and unchanged parts in the object beam will affect the visibility of the detected image. The dependence of the visibility on the ratio and the effect of a mixer were examined. For this purpose, a Twyman–Green interferometer was used, as shown in Fig. 8(a). The laser beam is divided into two beams by the beam splitter BS. One of them is reflected by the mirror M_1 mounted on a piezoelectric transducer PZT, and the beam size is limited in diameter by the aperture of d. The other is reflected by the fixed mirror M_2, and a part of the beam corresponding to the position of the aperture is blocked. They are put together with the beam splitter and become the object beam. Consequently, the incident object beam has two phase planes. We measured the response of the output object beam at the image plane. When the

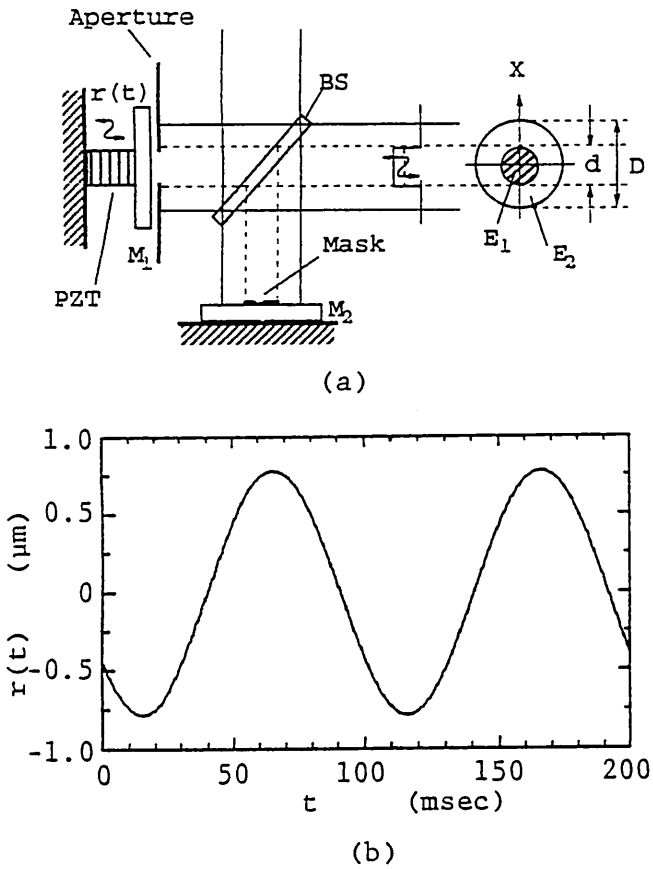

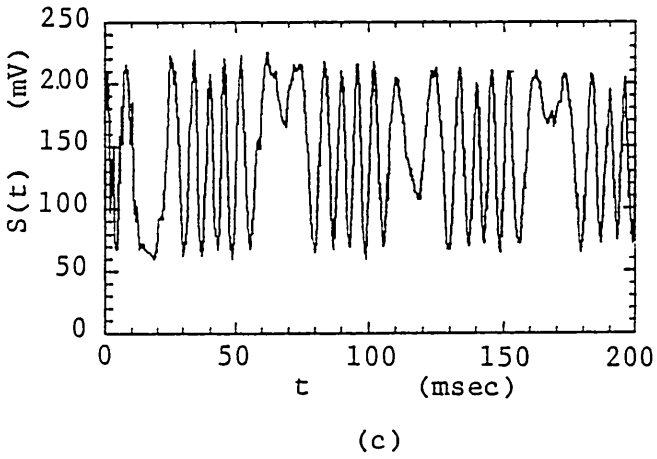

Fig. 8. Response of the output beam intensity for a phase change of the incident object beam. (a) Formation of the testing object beam. The phase in E_1 changes independently of that in E_2, (b) driving signal of the PZT, (c) measured interference signal at the image plane.

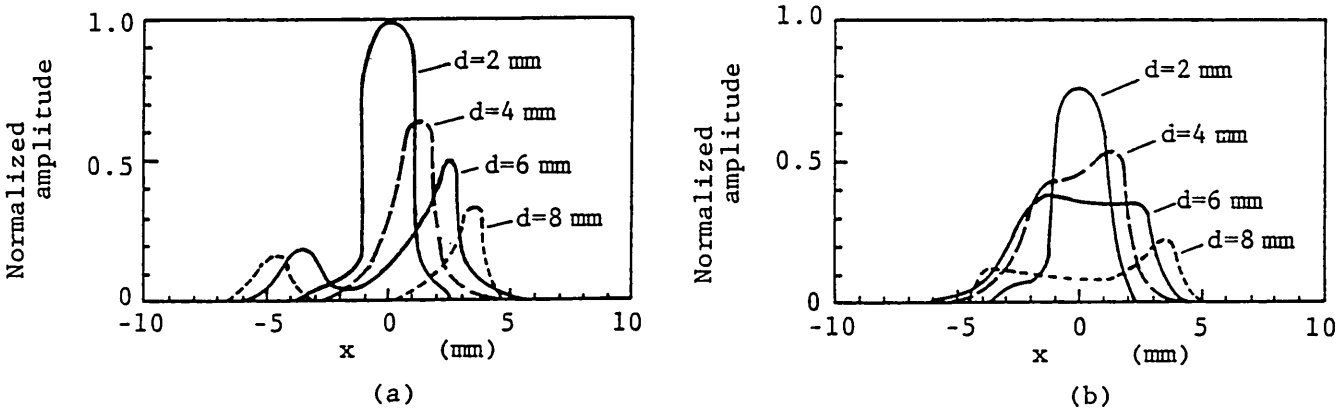

Fig. 9. Distributions of the amplitude of the interference signal $S(t)$ measured along the x axis (a) without a mixer and (b) with a mixer.

phase was changed by vibrating the PZT with a sinusoidal signal $r(t)$ of 10 Hz, as shown in Fig. 8(b), the output beam intensity $S(t)$ was observed as shown in Fig. 8(c). It is thought that the phase hologram is not destroyed during the measurement because the time constant τ is much larger than the period of phase change. The detected signal $S(t)$ is the result of interference of beams E_1 and E_2 at the image plane. The amplitude of $S(t)$ is observed by changing the diameter d. The results are shown in Fig. 9. Figure 9(a) is obtained without the mixer. It is asymmetric especially for $d > 4$ mm. This asymmetry is caused by the beam fanning, where most of the incident beam is diffracted in the positive x direction. Figure 9(b) shows the results obtained with the mixer. The amplitude is reduced slightly with the increase of d but is almost constant. This is the result of mixing beams E_1 and E_2.

C. Observation of Objects

Now we show some concrete images obtained by our system.

First, the refractive-index changes of the water were observed. The construction of the object and a shutter sequence is shown in Fig. 10. The water was heated partially only 1 s with a Nichrome wire. After that, the water around the Nichrome wire was observed every 5 s with or without a shutter. Figure 10 shows the observed results. The refractive index change in the water, in which the distribution of temperature differs from the other part, could be observed clearly when we used a shutter. Figure 10(b) shows refractive-index changes at $t = 5$ s and $t = 10$ s simultaneously. But we could not obtain the images without a shutter because the temperature in the water was changed too slowly.

Next, we show the observed result for the sinking opaque object in the water, obtained by using a shutter. The object is a ball approximately 4 mm in diameter. The object and the shutter sequence are shown in Fig. 11. The object was observed every 5 s with a shutter. The images in Figs. 11(a) and 11(b) were obtained without the mixer. The images at the position placed just before movement are detected

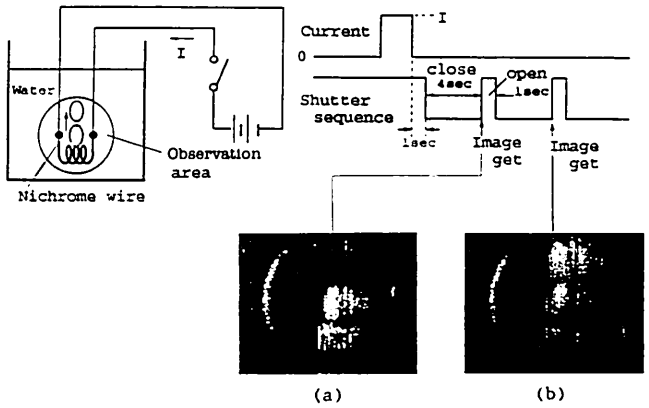

Fig. 10. Observation of the refractive-index change in the water when a shutter is used: (a) and (b) are images obtained at 5 and 10 s, respectively, after the electric current was broken.

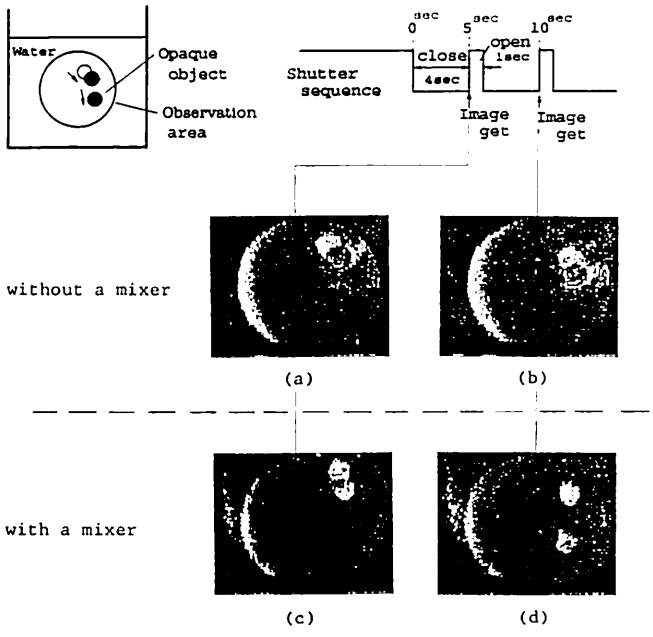

Fig. 11. Observation of the sinking opaque object in the water using a buffer: (a) and (b) are images observed without a mixer; (c) and (d) are images observed with a mixer.

clearly, but the images obtained after movement are clear only on the edge. The images obtained with the mixer are shown in Figs. 11(c) and 11(d). The intensity of the observed image is almost uniform.

IV. Conclusion

We have discussed the extended form of novelty imaging system using $BaTiO_3$ and a controlled shutter sequence by the examination of some experiments. The basic characteristics were examined for the sake of appropriate construction. It is confirmed that the shutter is useful in observing the slow-changing object, and we showed that the random phase plate is effective in measuring the opaque object clearly.

References

1. T. Kohonen, *Self-Organization and Associative Memory,* 2nd ed. (Springer-Verlag, New York, 1988), Chaps. 4 and 6.
2. T. Aida, K. Takizawa, and M. Okada, "Real-time tracking of a moving object in a television image using an optical system consisting of a liquid-crystal television and a position sensitive device," Opt. Lett. **14,** 835–837 (1989).
3. D. Z. Anderson, D. M. Lininger, and J. Feinberg, "Optical tracking novelty filter," Opt. Lett. **12,** 123–125 (1987).
4. M. Cronin-Golomb, A. M. Biernacki, C. Lin, and H. Kong, "Photorefractive time differentiation of coherent optical images," Opt. Lett. **12,** 1029–1031 (1987).
5. R. S. Cudney, R. M. Pierce, and J. Feinberg, "The transient detection microscope," Nature (London) **332,** 424–426 (1988).
6. N. Sze-Keung Kwong, Y. Tomita, and A. Yariv, "Optical tracking filter using transient energy coupling," J. Opt. Soc. Am. B **5,** 1788–1791 (1988).
7. F. Vachss and L. Hesselink, "Synthesis of a holographic image velocity filter using the nonlinear photorefractive effect," Appl. Opt. **27,** 2887–2894 (1988).
8. J. E. Ford, Y. Fainman, and S. H. Lee, "Time integrating interferometry using photorefractive fanout," Opt. Lett. **13,** 856–858 (1988).
9. D. T. H. Liu and L.-J. Cheng, "Resolution of a target-tracking optical novelty filter," Opt. Eng. **30,** 571–576 (1991).
10. J. Feinberg, "Asymmetric self-defocusing of an optical beam from the photorefractive effect," J. Opt. Soc. Am. **72,** 46–51 (1982).
11. R. A. Rupp and F. W. Drees, "Light-induced scattering in photorefractive crystals," Appl. Phys. B **39,** 223–229 (1986).
12. M. Cronin-Golomb and A. Yariv, "Optical limiters using photorefractive nonlinearities," J. Appl. Phys. **57,** 4906–4910 (1985).
13. M. B. Klein and G. C. Valley, "Beam coupling in $BaTiO_3$ at 442 nm," J. Appl. Phys. **57,** 4901–4905 (1985).
14. Ph. Refregier, L. Solymar, H. Rajbenbach, and J. P. Huignard, "Two-beam coupling in photorefractive $Bi_{12}SiO_{20}$ crystal with moving grating: theory and experiments," J. Appl. Phys. **58,** 45–57 (1985).
15. J. P. Huignard and A. Marrakchi, "Coherent signal beam amplification in two-wave mixing experiments with photorefractive $Bi_{12}SiO_{20}$ crystals," Opt. Commun. **38,** 249–254 (1981).
16. Y. Fainman, C. C. Guest, and S. H. Lee, "Optical digital logic operations by two-beam coupling in photorefractive materials," Appl. Opt. **25,** 1598–1603 (1986).
17. Y. Fainman, E. Klancnik, and S. H. Lee, "Optimal coherent image amplification by two-wave coupling in photorefractive $BaTiO_3$," Opt. Eng. **25,** 228–234 (1986).